Edge Learning Optimization in Task-Oriented NOMA Communications for Autonomous Vehicle Perception

Carla E. Garcia[1], Mario R. Camana[2], Abuzar B. Mohammad[1], Jorge Querol[1] and Symeon Chatzinotas[1]
[1]Interdisciplinary Centre for Security, Reliability and Trust (SnT), University of Luxembourg, Luxembourg City, Luxembourg
[2]School of Electrical Engineering, Korea University, Seoul, South Korea
Email: carla.garcia@uni.lu, mariocamana@korea.ac.kr, {abuzar.babikir, jorge.querol, symeon.chatzinotas}@uni.lu

2024 IEEE Wireless Communications and Networking Conference (WCNC) | 979-8-3503-0358-2/24/$31.00 ©2024 IEEE | DOI: 10.1109/WCNC57260.2024.10570514

***Abstract*—The Internet of Vehicles (IoV) is undergoing swift advancements in capability and intelligence, poised to facilitate a diverse range of innovative applications. Within the IoV, edge learning empowers intelligent applications and services by leveraging data-driven tasks. Therefore, in this paper, we propose optimizing the edge learning error prediction within an edge-supported Non-Orthogonal Multiple Access (NOMA) in task-oriented communications. Specifically, we consider three autonomous vehicle perception tasks, called: object detection, traffic sign, and weather classification. For this purpose, we propose a novel approach based on the Particle Swarm Optimization (PSO) algorithm to jointly minimize the edge learning error and optimize power allocation variables. Moreover, we investigate alternative benchmark schemes, including Quantum Particle Swarm Optimization, Cuckoo Search, and Butterfly Optimization algorithms. Satisfactorily, our simulations substantiate the superiority of the PSO algorithm over the baseline schemes, delivering superior performance with reduced computation time.**

***Index Terms*—task-oriented communication, edge learning, non-orthogonal multiple access (NOMA), learning error, particle swarm optimization (PSO).**

I. Introduction

The Internet of Vehicles (IoV) is a concept spurred by cutting-edge developments in vehicular communications to support a diverse range of intelligent IoV applications. These applications will blend fully autonomous vehicles, the Internet of Things (IoT), and the surrounding environment [1]. Therefore, within autonomous driving systems, perception plays a pivotal role in how a connected autonomous vehicle (CAV) comprehends its surroundings [1][2]. Moreover, the future of intelligent IoV heavily relies on strategic implementation of storage, edge caching, edge computing, and edge artificial intelligence (AI) technologies. In this sense, the emergence of edge computing as an alternative to traditional cloud computing addresses communication challenges posed by transmitting vast data volumes from diverse IoT devices to remote cloud servers [3][4].

In edge learning, the prime objective is extracting intelligence from dispersed data generated by subscribed IoT users. However, wireless channel issues become bottlenecks, particularly when transmitting substantial data volumes to an edge server, hindering ultra-fast edge learning [5]. Consequently, conventional data-centric communication systems relied on Shannon's theory to maximize network throughput, fall short in enhancing learning performance due to their reliance on classic source and channel coding theories. A paradigm shift to task-oriented communication, prioritizing learning performance over data transmission, becomes imperative [4] [6]. Task-oriented communication broadens the scope from micro-level assessments like bit or packet error rates to macro-level metrics such as learning rate and inference accuracy [7][8]. This approach reduces communication loads by transmitting only task-relevant information, like feature extraction for edge inference, rather than inundating networks with all observed data and disregarding structural information [7]. Research efforts such as [9] and [4] introduced strategies optimizing local feature extraction and power allocation within this task-oriented framework, focusing on eliminating redundant data transmission. Similarly, [10] proposed learning-centric power allocation (LCPA), emphasizing learning performance over communication throughput, showcasing superiority in classification error over conventional methods. To the best of our knowledge none of the aforementioned studies explored non-orthogonal multiple access (NOMA) to address spectrum scarcity issues arising from multiple connectivity in task-oriented communication systems for future wireless networks.

Motivated by the promising sector of autonomous driving, where achieving human-like perception is still a challenge due to open driving scenarios, and visual obstructions [2]. This this paper focuses on task-oriented communications within autonomous driving systems considering semantic and geometry perception for a multi-task scenario. Furthermore, motivated by the potential of NOMA and task-oriented communication systems, this paper investigates a low-complexity approach to jointly optimize learning error and power allocation for autonomous vehicle perception in an edge learning NOMA network.

Traditional optimization techniques striving to obtain the best solution often involve significant computational in-

979-8-3503-0358-2/24/$31.00 ©2024 IEEE

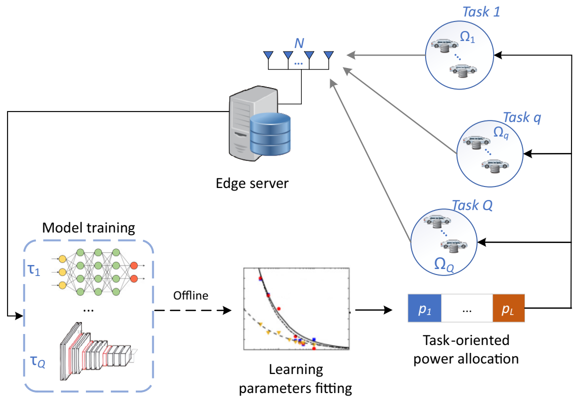

Fig. 1. The system model of NOMA for task-oriented edge learning.

tricacies, and a closed-form solution lacks adaptability, which require reformulation following any network alterations [11][12][13]. As a result, evolutionary computing algorithms within AI has emerged as a viable avenue for addressing intricate computational challenges. Consequently, this paper explores evolutionary computing techniques for jointly optimize power allocation and edge learning error in task-oriented communications with NOMA. Among these techniques, the particle swarm optimization (PSO)-based scheme demonstrates promise in balancing accuracy and computational complexity (CC) in a multi-task scenario. The remainder of the paper is organized as follows: Section II and Section III describes the system model and problem formulation, respectively. Section IV presents the proposed PSO framework. Section V provides the simulation results. Finally, Section VI concludes this paper.

II. System Model

Fig. 1 illustrates the proposed task-oriented communication in edge learning NOMA networks. The system model is composed of Q single-antenna user groups, with Q different learning tasks, $\{\tau_1, ..., \tau_Q\}$, and the edge server is equipped with N antennas. Let us define the group of users as $\Omega = \{\Omega_1, ..., \Omega_Q\}$, where Ω_q represents the users performing the q^{th} task, with the number of users equal to $|\Omega_q|$. The total number of users is denoted as L, i.e., $L = \sum\limits_{l=1}^{Q} |\Omega_q|$, and p_l denotes the power allocation for each l^{th} user. We assume each user is exclusively associated with a single task. Since we consider the number of user groups is equal to the number of Q different tasks [4].

In the Q multi-task learning shown in Fig. 1, each of these tasks contains a specific dataset, a learning model, the process of fine-tuning model parameters, and a task-oriented power assignment. Moreover, $\mathbf{g}_l \in \mathbb{C}^{N\times 1}$ denotes the complex-valued channel fast-fading vector from the l^{th}user to the edge server. It is assumed that users in a higher indexed group have better channel conditions than users in a lower indexed group. Without loss of generality, we consider $\|\mathbf{g}_1\|^2 \leq, ..., \leq \|\mathbf{g}_L\|^2$. In uplink NOMA, the decoding process performed by the successive interference cancellation (SIC) technique, prioritizes channels in descending order of power [14]. This means the signal with the highest power and linked with the L^{th} user is decoded first at the edge server. Consequently, this initial decoding encompasses interference from all users that have comparatively weaker channel conditions. Accordingly, the achievable rate of decoding a message from the l^{th} user can be expressed as follows:

$$R_l^{NOMA} = \begin{cases} \log_2\left(1 + \frac{p_l h_{l,l}}{\sum\limits_{j=1, j\neq l}^{l-1} p_j h_{l,j} + \sigma^2}\right), 2 \leq l \leq L \\ \log_2\left(1 + \frac{p_l h_{l,l}}{\sigma^2}\right), l = 1 \end{cases}, \tag{1}$$

where $h_{l,j}$ represents the composite channel gain from the j^{th} user at the edge server when decoding data of the l^{th} user, computed as $h_{l,l} = \delta_l \|\mathbf{g}_l\|_2^2$ if $j = l$, and $h_{l,j} = \delta_j \left|\mathbf{g}_k^H \mathbf{g}_j\right|^2 \Big/ \|\mathbf{g}_k\|_2^2$ if $j \neq l$. δ_l is the path loss of the l^{th} user, and σ^2 denotes the variance of additive white Gaussian noise.

On the other hand, by using maximum ratio combining (MRC) without applying NOMA, interference from other users is considered noise. Subsequently, the achievable data rate of the l^{th}user can be written as follows:

$$R_l^{MRC} = \log_2\left(1 + \frac{p_l h_{l,l}}{\sum\limits_{j=1, j\neq l}^{L} p_j h_{l,j} + \sigma^2}\right). \tag{2}$$

At the edge server, the number of samples conveyed by a user to learn task τ_q can be computed as follows [1]:

$$S_q = \sum_{l\in\Omega_q} \left\lceil \frac{BTR_l^{NOMA}}{V_q} \right\rceil + D_q \approx \sum_{l\in\Omega_q} \frac{BTR_l^{NOMA}}{V_q} + D_q, \tag{3}$$

where the total bandwidth in hertz is denoted by B, and T is the transmission time in seconds. Moreover, for the q^{th} pre-trained task, D_q denotes the initial amount of historical data and V_q represents the number of bits. Furthermore, a nonlinear exponential function, $\Theta_q\left(S_q \left| a_q, b_q\right.\right) \triangleq a_q S_q^{-b_q}$, is formulated to represent the characteristics of the learning error function, where the tuning parameters a_q and b_q represent non-independent and identically distributed parallel datasets, respectively. Note that this expression is given in order to link wireless resource assignment with the performance of machine learning. In practice, values for a_q and b_q are set through a process of fitting the learning error function from the historical dataset. This tuning function closely aligns with the empirical data of the machine learning model, demonstrating a strong correlation [4].

III. Problem Formulation

In this paper, our aim is to minimize the learning error function by jointly optimizing the power allocation variables in the proposed task-oriented communication in edge learning NOMA network for multi-users. Moreover, we consider a multi-task scenario. Therefore, the optimization problem is formulated as follows:

$$\min_{\{p_l\}} \quad \sum_{q=1}^{Q} \phi_q \times a_q S_q^{-b_q} \tag{4a}$$

$$\text{s.t.} \quad \sum_{l=1}^{L} p_l = P_{\max}, \tag{4b}$$

$$p_l \geq 0, \forall_l \in \Omega, \tag{4c}$$

where $\phi_q \triangleq D_q V_q \Big/ \left(\sum_{i=1}^{Q} D_i V_i \right)$ is the weight of diverse datasets, and $P_{\max}$ is the power budget that the sum of all scheduled users shall satisfy [4].

Note that the objective function in (4) is able to adapt to diverse learning tasks through the dynamic adjustment of weight factors $\phi_q, \forall q$. For the single-task case (SC), the objective function can be expressed by $a_{SC} S_{SC}^{-b_{SC}}$.

In addition, as a comparative approach, we formulate the optimization problem for the conventional sum-rate maximization as follows:

$$\max_{\{p_l\}} \sum_{l=1}^{L} R_l^{NOMA} \tag{5a}$$

$$\text{s.t.} \quad (4b), (4c). \tag{5b}$$

IV. PSO-Based Optimization Scheme

The PSO algorithm stands as a promising optimization scheme rooted in a population framework called the swarm. This collective comprises particles that navigate through a search space with the primary goal of discovering the optimal solution. The variables to be optimized are in each particle, and the position of each particle position undergoes continuous updates in every iteration, oriented to both local and global best positions. The global best position corresponds to the position within the population where a particle achieves the highest yield, considering the collective performance. Conversely, the local best position reflects the individual best position attained by a particle thus far in its exploration. In this study, each particle position is represented by $\mathbf{e}_m$, it is a vector of the variables $(p_1, p_2, ..., p_L)$ to be optimized, as follows:

$$\mathbf{e}_m = \{e_{p_1,m}, e_{p_2,m}, ..., e_{p_L,m}\} \tag{6}$$

where $m = 1, 2, 3, ..., M^{PSO}$, and M^{PSO} is the number of particles in the swarm. Then, the search region for each variable of the particle's position, $e_{p_1,m}, e_{p_2,m}, ..., e_{p_L,m}$ is denoted as $[0, P_{\max}]$.

Since the proposed problem (4) entails constrained optimization, it requires a method to address these constraints. Hence, we employ the penalty method, wherein the fitness function $F(\mathbf{e}_m) = F(e_1, e_2, ..., e_m)$ is derived based on the cost function indicated in (4), as follows:

$$F(\mathbf{e}_m) = f(\mathbf{e}_m) + \psi\omega, \tag{7}$$

where ψ is the penalty value, ω is defined based on the constraint (4b), and $\omega = 0$ if constraint (4b) is satisfied, whereas $\omega = 1$, otherwise. $f(\mathbf{e}_m)$ is the objective function (4a) evaluated with $\mathbf{e}_m = \{e_{p_1,m}, e_{p_2,m}, ..., e_{p_L,m}\}$.

Algorithm 1 The proposed PSO scheme to solve problem (4).

1: Set the input parameters and the iteration count $t = 1$.
2: Initialize positions and velocities of the particles.
3: Calculate minimum learning error by $f(\mathbf{e}_m)$.
4: Calculate the initial $\mathbf{lb}_m^t$, $\forall m$, i.e., $\mathbf{lb}_m^t = \mathbf{e}_m^t$.
5: Evaluate $\mathbf{gb}^t = \underset{1 \leq m \leq M^{PSO}}{\arg\min} \; f\left(\mathbf{lb}_m^t\right)$.
6: **For** each particle m **do**
7: Compute (8) for update the velocities.
8: Compute (9) for the positions updating.
9: Compute the new best particles' positions,
if $f\left(\mathbf{e}_m^{t+1}\right) < f\left(\mathbf{lb}_m^t\right)$ **then** $\mathbf{lb}_m^{t+1} = \mathbf{e}_m^{t+1}$
else $\mathbf{lb}_m^{t+1} = \mathbf{lb}_m^t$
end if
10: **end for**
11: Compute the new global best particles' positions,
$\mathbf{gb}^{t+1} = \underset{1 \leq m \leq M^{PSO}}{\arg\min} \; f\left(\mathbf{lb}_m^{t+1}\right)$.
12: **if** $t < M^{PSO}$ **then** $t = t + 1$ and go to stage 6
else go to Step 13
end if
13: **Return:** the best values of power allocation variables, $\{p_1^*, p_2^*, ..., p_L^*\} = \mathbf{gb}$, in problem (4).

Moreover, the search strategy employed to determine the optimal solution relies on updating the velocity and position of each particle. The updating of the particle velocities can be expressed as follows:

$$\mathbf{v}_m^{t+1} = In^t \mathbf{v}_m^t + j_1 c_1 \left(\mathbf{lb}_m^t - \mathbf{e}_m^t\right) + j_2 c_2 \left(\mathbf{gb}^t - \mathbf{e}_m^t\right), \tag{8}$$

where the inertia weight is denoted by In, the velocity of the m-th particle in the t^{th} iteration is denoted by v_m^t, $\mathbf{e}_m^t$ denotes the position of the m^{th} particle in the t^{th} iteration. The global best position and the local best are denoted by $\mathbf{gb}^t$, and $\mathbf{lb}_m$, respectively. j_1 and j_2 are random numbers between 0 and 1, and c_1, and c_2 are the cognitive and social parameters, respectively.

Next, the position of the m^{th} particle is updated based on the elements outlined in (6), the previous particle position along with the velocity derived from (8), as follows:

$$\mathbf{e}_m^{t+1} = \mathbf{e}_m^t + \mathbf{v}_m^{t+1}. \tag{9}$$

Algorithm 1 describes the proposed PSO scheme. The input parameters pf the proposed PSO-base scheme encompass $P_{\max}$, M^{PSO}, In, j_1, j_2, c_1, c_2, and the maximum number of iterations, denoted by I^{PSO}. Furthermore, the initial global best position is determined based on the cost function of problem (4). In this study, the initial $\mathbf{gb}$ selection involves choosing the minimum value in the cost function among all the initial particle positions.

V. Simulation Results

In this section, we present the simulation results to evaluate the performance of our devised schemes against benchmark methods. The wireless communication parameters were configured akin to those specified in [10]. In particular, we set the communication bandwidth equal to $B = 180\text{kHz}$, the number of users $L = 6$, the power budget, $P_{\max} = 20\text{mW}$, and the path loss for each user, $\delta_l = -90\text{dB}$, and the wireless channel, $\mathcal{CN}\left(0, \delta_l \mathbf{I}\right)$.

We deem three tasks, one for each set of users (i.e., three user sets). Each task corresponds to a distinct user set, comprising two users per set. Therefore, in our exploration of task-oriented learning at the edge NOMA networks, we investigated three specific tasks pertinent to autonomous driving [2]:

- Task 1: Weather classification utilizing RGB images and a Convolutional Neural Network (CNN), with $V_1 = 0.7\text{MB}, \text{D}_1 = 300$,
- Task 2: Object detection employing point cloud data and Sparsely Embedded Convolutional Detection (SECOND), with $V_2 = 1.6\text{MB}, \text{D}_2 = 300$,
- Task 3: Traffic sign using RGB images and YOLOV5, with $V_3 = 0.7\text{MB}, \text{D}_3 = 300$,

The results were averaged over several channel realizations. Datasets collected for these experiments were generated by the open-source autonomous driving simulation platform called CarlaFLCAV. The datasets used in our analysis can be accessed online at https://github.com/SIAT INVS/CarlaFLCAV [2][4].

In the simulations, we considered the swarm-intelligence schemes: PSO, QPSO, CS, and BOA [15]. The parameters for each scheme were established through an analysis of optimal outcomes derived from multiple experiments. Then, the values of the parameters for PSO are equal to $M^{PSO} = 55$, $I^{PSO} = 500$, $In = 0.7$, and $c_1 = c_2 = 1.496$. For QPSO, the simulation parameters are equal to $M^{QPSO} = 55$, $I^{QPSO} = 500$. For CS, the simulation parameters are equal to $M^{CS} = 55$, $I^{CS} = 500$, the probability of abandoned maximum and minimum are $p_a^{\max} = 0.5$, and $p_a^{\min} = 0.25$, respectively. For BOA, the number of agents, the number of generations, the sensory modality, the power exponent, and the switch probability are equal to $S^{BOA} = 70$, $G^{BOA} = 500$, $se = 0.01$, $px = 0.01$, $sw = 0.5$, respectively.

Fig. 2 illustrates the convergence behavior for the multiple-task case of the proposed PSO algorithm alongside three other swarm intelligence baseline schemes, called: CS, QPSO, and BOA. Here, the number of antennas is equal to $N = 6$, and the variance of additive white Gaussian noise is $\sigma = -90\text{dBm}$. The learning error is calculated based on (4a). From Fig. 2, it can be observed that with an increase in the number of iterations, there is a decrease in the learning error. Therefore, the PSO exhibits a swifter convergence compared to the other swarm-learning algorithms, demonstrating superior performance over CS, QPSO, and BOA in terms of convergence speed. Moreover, we can observe that the PSO algorithm and the CS scheme achieve the lowest learning error.

To ascertain the superiority of the PSO algorithm compared to the CS baseline scheme, we conducted evaluations based on CC and computation time. Specifically, the CC of PSO relies on M^{PSO}, and I^{PSO}. Consequently, its CC is expressed as

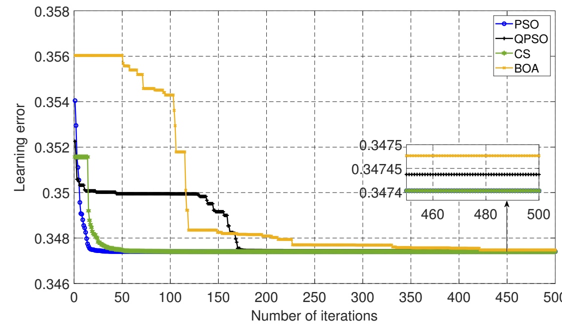

Fig. 2. Convergence behavior of the swarm intelligence algorithms for the proposed edge learning task-oriented communications with NOMA.

$\mathcal{O}\left(M^{PSO} \cdot I^{PSO}\right)$. Meanwhile, the CC of CS is based on the number of nests, M^{CS}, the probability of abandonment, pa, and the number of iterations, I^{CS}. Accordingly, the CC for CS is given by $\mathcal{O}\left(\left(M^{CS} + \left(pa \cdot M^{CS}\right)\right) \cdot I^{CS}\right)$. Therefore, we confirm that the PSO algorithm attains lower computational complexity. This is primarily due to the lack of a probability factor in its CC, a factor that is present in the complexity of the CS algorithm. Furthermore, within the CC of CS, this factor is multiplied by the number of particles, resulting in a slower resolution time compared to that required by PSO. In addition, the computational time obtained by PSO,QPSO,CS, and BOA are equal to 1.288s, 3.613s, 2.546s, and 2.94s, respectively, for the learning error values show in Fig. 2. Thus, while the learning error performance show marginal differences across the algorithms, the primary distinction lies in computational time. As a result, the least computation time is obtained by the proposed PSO.

To gain more insight of the benefits of multi-antenna in the proposed task-oriented communication with NOMA transmission strategy, Fig. 3 and Fig. 4 show the learning error and sum rate versus the number of antennas, respectively. We consider two values for the variance of additive white Gaussian noise: $\sigma = -80\text{dBm}$ and $\sigma = -90\text{dBm}$. From Fig. 3, we can observe that as the number of antennas increased the learning error decreased. Moreover, from Fig. 6 we can observe that the sum rate is improved by employing a greater number of antennas. Overall, this improvement is particularly attributable to the spatial diversity benefits derived from the utilization of multiple antennas. Furthermore, from Fig. 3 and Fig. 4, we observe that NOMA overcomes MRC in both, sum rate and learning error performance.

Fig. 5 illustrates the correlation between learning error and power budget within our proposed approach outlined in equation (4), aimed at minimizing learning error. Contrarily, the baseline scheme in (5) primarily targets the conventional objective of maximizing the sum rate. Fig. 5 showcases a consistent trend across various scenarios: an increase in the power budget leads to a decrease in learning error. This is because by augmenting the overall available power, a larger power reservoir becomes accessible for transmitting data from users to the edge server. This leads to an increase in the

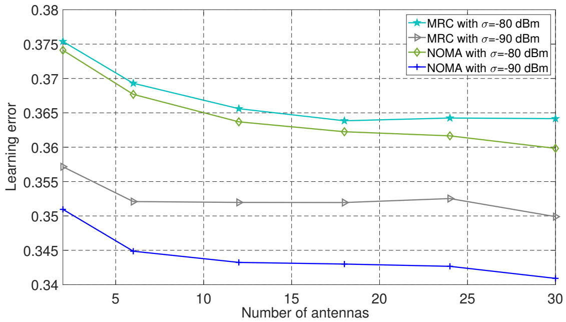

Fig. 3. Learning error versus number of antennas between the proposed edge learning task-oriented communications with NOMA and the baseline with MRC.

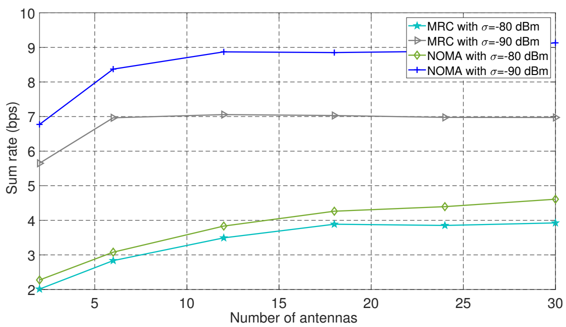

Fig. 4. Sum rate versus transmission power in edge learning task-oriented communications with NOMA.

achievable rate, thereby reducing the learning error captured by the objective function. Note that according to (1) and (2), an increase in the sum rate aligns with a decrease in the learning error. Moreover, another insight arises when comparing these two methodologies. Our optimization problem described in (4) surpasses the conventional sum-rate maximization approach described in (5) by achieving a lower learning error. This advantage is attributed to the integration of learning parameters such as the number of the historical data D_i, the bit number of each data V_i, and a_q, b_q from the historical dataset by fitting the cost function, into the optimization problem. These components overlooked by the sum-rate maximization scheme in equation (5).

VI. Conclusion

In this paper, we propose a novel approach based on PSO to jointly optimize a power allocation and edge learning error within a task-oriented edge NOMA system, specifically for an autonomous vehicle perception in multi-task scenario. Our proposed PSO-based approach provides a low-complexity solution with a low learning error, compared to other swarm learning techniques. Moreover, simulation results show that the PSO algorithm demonstrates superior performance while demanding less computation time than its counterparts. Additionally, simulation results confirm that integrating NOMA into the proposed task-oriented edge learning system yields

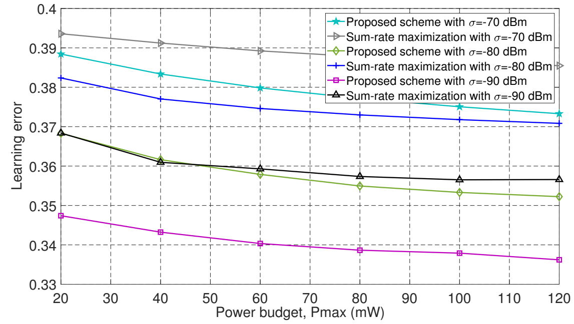

Fig. 5. Learning error versus power budget between the proposed edge learning error optimization and the conventional sum rate maximization scheme.

higher achievable data rates than those achieved through conventional MRC method.

VII. Acknowledgments

This work was supported by the SIGCOM research group of the Interdisciplinary Center for Security, Reliability and Trust (SnT) of the University of Luxembourg, Luxembourg.

References

[1] J. Zhang and K. B. Letaief, "Mobile Edge Intelligence and Computing for the Internet of Vehicles," Proceedings of the IEEE, vol. 108, no. 2, pp. 246–261, Feb. 2020,

[2] S. Wang et al., "Federated Deep Learning Meets Autonomous Vehicle Perception: Design and Verification," *IEEE Network*, vol. 37, no. 3, pp. 16–25, May 2023.

[3] A. Nüchter, R. B. Rusu, D. Holz, and D. Munoz, "Semantic perception, mapping and exploration," *Robotics and Autonomous Systems*, vol. 62, no. 5, pp. 617–618, May 2014.

[4] H. Xie, M. Xia, P. Wu, S. Wang, and H. V. Poor, "Edge Learning for Large-Scale Internet of Things With Task-Oriented Efficient Communication," *IEEE Transactions on Wireless Communications*, pp. 1–1, 2023.

[5] K. B. Letaief, Y. Shi, J. Lu, and J. Lu, "Edge Artificial Intelligence for 6G: Vision, Enabling Technologies, and Applications," *IEEE Journal on Selected Areas in Communications*, vol. 40, no. 1, pp. 5–36, Jan. 2022.

[6] E. Li, L. Zeng, Z. Zhou, and X. Chen, "Edge AI: On-Demand Accelerating Deep Neural Network Inference via Edge Computing," *IEEE Transactions on Wireless Communications*, vol. 19, no. 1, pp. 447–457, Jan. 2020.

[7] Y. Shi, Y. Zhou, D. Wen, Y. Wu, C. Jiang, and K. B. Letaief, "Task-Oriented Communications for 6G: Vision, Principles, and Technologies," *IEEE Wireless Communications*, vol. 30, no. 3, pp. 78–85, Jun. 2023.

[8] A. Mostaani, T. X. Vu, S. K. Sharma, V.-D. Nguyen, Q. Liao, and S. Chatzinotas, "Task-Oriented Communication Design in Cyber-Physical Systems: A Survey on Theory and Applications," *IEEE Access*, vol. 10, pp. 133842–133868, 2022

[9] J. Shao, Y. Mao, and J. Zhang, "Task-Oriented Communication for Multidevice Cooperative Edge Inference," *IEEE Transactions on Wireless Communications*, vol. 22, no. 1, pp. 73–87, Jan. 2023.

[10] S. Wang et al., "Federated Deep Learning Meets Autonomous Vehicle Perception: Design and Verification," *IEEE Network*, vol. 37, no. 3, pp. 16–25, May 2023.

[11] C. E. Garcia, M. R. Camana and I. Koo, "Ensemble Learning Aided QPSO-Based Framework for Secrecy Energy Efficiency in FD CR-NOMA Systems," in *IEEE Transactions on Green Communications and Networking*, vol. 7, no. 2, pp. 649-667, June 2023.

[12] M. J. Mohiz, N. K. Baloch, F. Hussain, S. Saleem, Y. B. Zikria, and H. Yu, "Application mapping using cuckoo search optimization with Lévy flight for NoC-based system," *IEEE Access*, vol. 9, pp. 141778–141789, 2021.

[13] Maldonado, D. et al., "Optimum frequency response with decentralized drivers in power system," *IET Generation, Transmission & Distribution*, vol. 17, pp. 1985–1998, 2023.

[14] C. E. Garcia, M. R. Camana, and I. Koo, “Joint Beamforming and Artificial Noise Optimization for Secure Transmissions in MISO-NOMA Cognitive Radio System with SWIPT,” Electronics, vol. 9, no. 11, p. 1948, Nov. 2020.
[15] M. O. Okwu and L. K. Tartibu, Metaheuristic Optimization: NatureInspired Algorithms Swarm and Computational Intelligence, Theory and Applications, vol. 927. Cham, Switzerland: Springer, 2020.